Nuclear Instruments and Methods in Physics Research A ▮ (▮▮▮▮) ▮▮▮–▮▮▮

Contents lists available at ScienceDirect

Nuclear Instruments and Methods in Physics Research A

journal homepage: www.elsevier.com/locate/nima

High-rate performance of the MWPCs for the LHCb muon system

M. Anelli [a], V. Bocci [b], G. Chiodi [b], P. Ciambrone [a], E. Dané [a], G. Felici [a], C. Forti [a], M. Gatta [a], F. Iacoangeli [b], G. Lanfranchi [a], G. Martellotti [b], R. Nobrega [b], G. Penso [c], D. Pinci [b,*], W. Rinaldi [b], R. Rosellini [a], M. Santoni [a], A. Saputi [a], A. Sarti [a], B. Sciascia [a]

[a] INFN, Laboratori Nazionali di Frascati, Italy
[b] INFN, sezione di Roma, Italy
[c] Università di Roma "La Sapienza" and INFN, Roma, Italy

ARTICLE INFO

Article history:
Received 15 April 2008
Received in revised form
16 May 2008
Accepted 25 May 2008

Keywords:
Gas detectors
Multiwire proportional chambers
Tracking and position-sensitive detectors
Elementary-particle and nuclear physics experimental methods and instrumentation

ABSTRACT

The high-rate performance of a multiwire proportional chamber of the LHCb muon detector was tested. The chamber, equipped with the final front-end electronics, was tested using a ~100 GeV muon beam superimposed on a 662 keV γ flux of variable intensity produced by the ^{137}Cs radioactive source of the CERN Gamma Irradiation Facility (GIF). No significant variation in the muon detection efficiency or in the time response of the chamber was observed at the highest gamma rate.

1. Introduction

The LHCb muon system [1–3] that will operate at the Large Hadron Collider (LHC) at CERN consists of five tracking stations (M1–M5) placed along the beam axis. Each station is divided into four regions (R1–R4) according to their distance from the beam axis. The station M1, placed in front of the electromagnetic and hadronic calorimeters, is equipped with 12 GEM chambers [4–8] in region R1 (near the beam pipe) and with 264 two-gap Multiwire Proportional Chambers (MWPCs) in regions R2–R4. The remaining four stations (M2–M5) comprise 1104 four-gap MWPCs [9–11]. In all MWPCs the anode wire planes are centered in a 5 mm gas gap and consist of 30 μm diameter gold-plated tungsten wires [12] with 2 mm spacing.

In this paper we report a high-rate test of a MWPC of the muon detector. The test was performed at CERN with the Gamma Irradiation Facility (GIF) [13,14]. The chamber we tested belongs to region R3 of station M3. As the gap geometry is identical for all chambers, the results presented in the following are valid for all the MWPCs of the muon detector.

2. Experimental setup

The MWPC we tested is composed [15,16] of four gaps (A, B, C and D in Fig. 1). The chamber was flushed with a $CO_2/Ar/CF_4$ gas mixture, 40/40/20% in volume. In each gap of the chamber, one of the two cathode planes is divided in 48 × 2 pads of 2.7 × 13.5 cm^2. Each pad of gap A (C) is hard-wired (Fig. 1) with the corresponding pad of gap B (D). This defines the physical channel AB (CD) which is read out by a channel of the front-end electronics (FEE). The outputs of the FEE of two corresponding physical channels AB and CD are logically OR-ed on the FEE board and provide a logical channel. The read-out system of the tested MWPC thus comprises 192 physical channels and 96 logical channels.

During the test, the four gaps were supplied by four independent high-voltage (HV) lines. This allowed us to study the chamber in three different configurations:

- The "four-gap" configuration: the four gaps (A, B, C and D) are supplied at the same HV value. This will be the standard configuration in the experiment.
- The "two single-gap" configuration: two gaps (AC or BD) read out by two different FEE channels (Fig. 1) are set at the same HV, while the other gaps (BD or AC, respectively) are switched off. This configuration simulates a chamber of the M1 station, where the MWPCs comprise two gaps, each one being read by

* Corresponding author.
E-mail address: davide.pinci@roma1.infn.it (D. Pinci).

0168-9002/$ - see front matter © 2008 Elsevier B.V. All rights reserved.
doi:10.1016/j.nima.2008.05.046

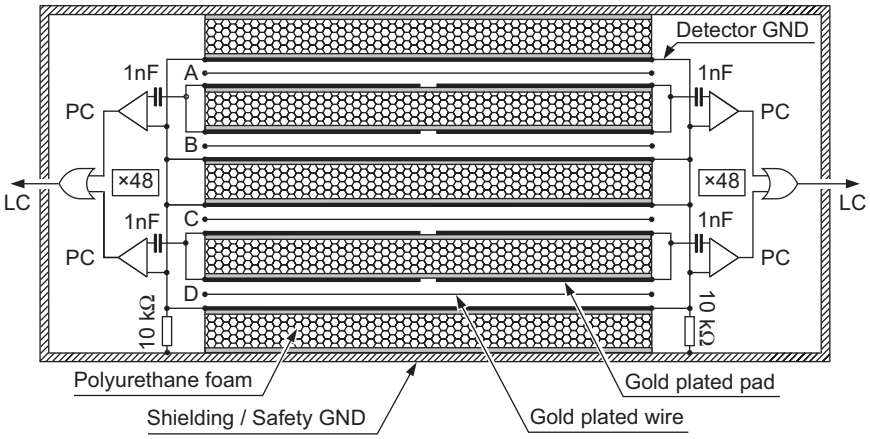

Fig. 1. Cross-section of the four-gap MWPC we tested. The four anode wire planes in gaps A, B, C and D were supplied by four independent high voltage (HV) lines. In each gap a cathode plane is segmented in 48 pairs of pads. Two corresponding pads in gaps A (C) and B (D) are hard-wired and define a physical channel (PC). The OR of two corresponding physical channels defines a logical channel (LC).

a different FEE channel (Fig. 1).

- The "one double-gap" configuration: two adjacent gaps (AB or CD), read out by the same FEE channel (Fig. 1), are set at the same HV value, while the other two gaps (CD or AB, respectively) are switched off. This configuration simulates a four-gap chamber which operates as a double-gap because of a FEE failure.

The MWPC was equipped with the final version of the FEE. The read-out electronics was mounted on 12 CARDIAC[1] boards fixed to the chamber. Each board comprised two CARIOCA[2] chips and one DIALOG[3] chip. The CARIOCA [17] is an application-specific integrated circuit (ASIC) comprising 8 amplifier–shaper–discriminators with base-line restoration. The DIALOG [18,19] is an ASIC with 16 input channels and 8 output channels. During the test, it performed the logical combination of eight pairs of physical channels into eight logical channels. It also makes it possible to control the two CARIOCAs mounted on the same board and to synchronize and count the pulses of the physical channels. The FEE was monitored and calibrated by a Service Board (SB) system [20,21].

The MWPC was placed in the experimental area (Fig. 2) of the GIF [13,14] where it was simultaneously exposed to a ~100 GeV muon beam and to the 662 keV photon flux coming from a 630 GBq (at the time of the test) ^{137}Cs radioactive source.

The photon flux could be varied by inserting different absorbing filters in front of the source. These filters were specially shaped to obtain a uniform gamma flux over the entire chamber surface. In the measurements presented in this paper only one filter was retained so that the MWPC was tested with the maximum obtainable uniform gamma flux.

The muons defined by a coincidence between the scintillators S_1, S_2, S_3 and S_4 (Fig. 2) are detected by the MWPC with (source "ON") and without (source "OFF") the photon flux. This allows us to test the detection efficiency and the time resolution of the MWPC in the presence of a high-rate background.

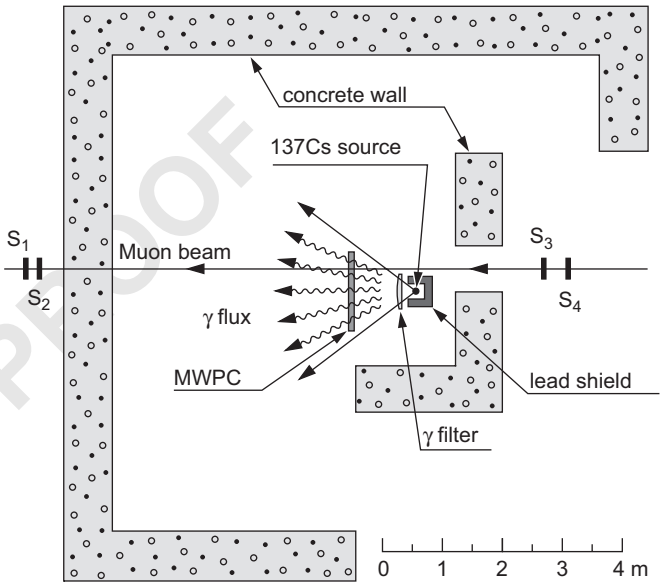

Fig. 2. Setup of the test. The MWPC is exposed to the gamma emitted by the ^{137}Cs source and to the muon beam which is monitored by the scintillators S_1-S_4.

3. Measurements and results

3.1. Measurements with the radioactive source

The measurements performed with the radioactive source and without the muon beam test the behavior of the MWPC without the FEE. The current drawn by each gap of the chamber, in the "four-gap" configuration, was measured as a function of the chamber HV. The 662 keV photons from the ^{137}Cs source are absorbed weakly when passing through the chamber, so that the photon flux is, to within a few percent, the same on each of the four gaps. The results of these measurements are reported in Fig. 3a. For all the HV values the currents in the four gaps differ less than ±20% in agreement with the expected gain tolerance [22]. In Fig. 3b (upper curve) the current density averaged on the four gaps of the MWPC is shown as a function of the HV. For comparison we report in the same chart (lower curve) the measurements [11] recorded on a similar chamber, with a much lower intensity ^{137}Cs source. The similar behavior of the two

[1] CARioca and DIAlog Circuits.
[2] Cern And RIO Current Amplifier.
[3] DIagnostic, time Adjustment and LOGics.

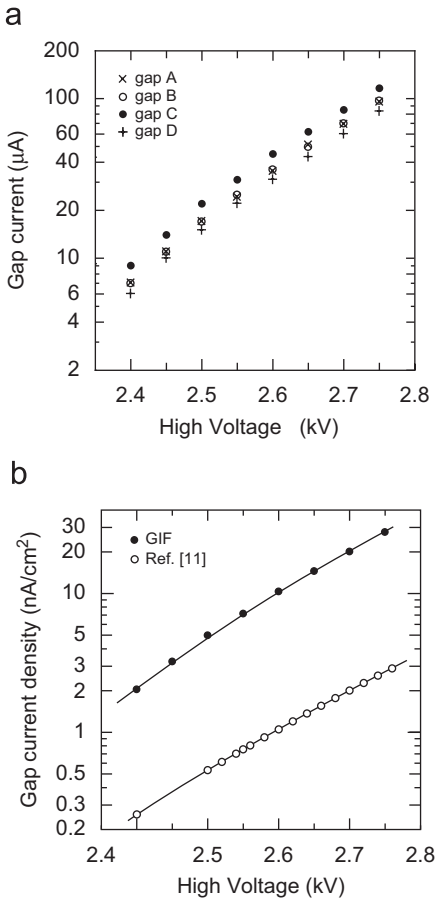

Fig. 3. (a) Current drawn by each gap with the GIF source ON, as a function of the chamber high voltage. (b) Current density averaged on the four gaps as a function of the high voltage; upper curve: measured at the GIF with the source ON; lower curve: measured with a lower intensity ^{137}Cs source [11].

Table 1
Current density (nA/cm^2) in a gap of the MWPCs, expected at the LHC with a luminosity of 2×10^{32} cm^{-2} s^{-1} and no safety factor

Average current density (nA/cm^2) in the most irradiated chamber (in the most irradiated cm^2)				
	R1	R2	R3	R4
M1	– –	15.0 ± 0.9 (32.4 ± 1.8)	5.69 ± 0.45 (12.7 ± 0.8)	3.18 ± 0.36 (6.19 ± 0.45)
M2	5.90 ± 0.41 (12.2 ± 0.7)	1.96 ± 0.18 (4.72 ± 0.31)	0.43 ± 0.08 (1.68 ± 0.15)	0.14 ± 0.04 (0.70 ± 0.09)
M3	1.38 ± 0.12 (5.54 ± 0.37)	0.39 ± 0.06 (1.48 ± 0.14)	0.12 ± 0.03 (0.74 ± 0.09)	0.04 ± 0.01 (0.49 ± 0.09)
M4	1.0 ± 0.11 (4.43 ± 0.30)	0.30 ± 0.05 (1.52 ± 0.14)	0.09 ± 0.03 (0.74 ± 0.09)	0.03 ± 0.01 (0.45 ± 0.08)
M5	0.65 ± 0.07 (2.99 ± 0.22)	0.18 ± 0.03 (1.27 ± 0.14)	0.08 ± 0.03 (0.78 ± 0.09)	0.02 ± 0.01 (0.49 ± 0.09)

The current densities are averaged on the most irradiated chambers (in the most irradiated cm^2) of the different regions (R1–R4) and stations (M1–M5) of the muon system. The data refer to a gas mixture of $CO_2/Ar/CF_4$, 55/40/5% in volume and to gain of 7.0×10^4 corresponding [11] to a HV of 2.6 kV. In region R1 of station M1 the muon detector is composed of GEM chambers.

curves[4] ensures that no evident saturation effect is present up to a current density of 28 nA/cm^2.

To evaluate the significance of this result, the maximum current density reached at the GIF must be compared with the values expected at the LHC, in the different regions of the muon detector. These values were calculated taking into account the local particle rate, the ionization produced by a charged particle crossing the gas gap and the gain of the chambers. The local particle rate was estimated [23] from a Monte Carlo sample of minimum bias events, assuming a luminosity of 2×10^{32} cm^2/s and no safety factor. The ionization of a minimum ionizing particle traversing the 5 mm gas gap, calculated [22] with HEED [24], is for the final gas mixture $\sim 36 \pm 2$ electrons–ions pairs. The gain of a MWPC was measured precisely [11] as a function of the HV. At the working voltage of the chamber (2.60–2.65 kV) the gain varies from 7.0×10^4 to 9.7×10^4. The current density expected in the different regions of the muon detector was calculated from these data. The results, summarized in Table 1, show that in all the chambers of the muon detector the average current density is below the value of 28 nA/cm^2 tested at the GIF. Only in the most irradiated cm^2 in region R2 of station M1 the expected current density is slightly larger than the tested value. No significant space charge effect is therefore expected at the LHC in the MWPCs of the muon detector.

3.2. Measurements with the radioactive source and the muon beam

To test the chamber and its FEE, the detection efficiency and the time resolution of this system were measured with crossing muons and with the source ON and OFF.

3.2.1. Detection efficiency

The detection efficiency of the chamber in a 20 ns time window was measured at different chamber HV. In Fig. 4 we report the results for the three chamber configurations and for the source ON and OFF. In all the configurations, a lower detection efficiency is observed (full points of Fig. 4) when the chamber is exposed to the gamma flux. This is expected because of the dead time of the FEE. To establish whether other causes are also present, the effect of the dead time on the chamber efficiency was evaluated taking into account the counting rate of a single logical channel when the gamma flux is present (Fig. 5) and the electronics pulse width that determines the dead time of a single channel. Because the signals delivered by the "low-energy" photons of the ^{137}Cs source in the four gaps are uncorrelated, the muon detection inefficiency due to the electronics dead time is different in the three chamber configurations. In the "four-gap" and in the "two single-gap" configurations the crossing muon is detected by two front-end CARIOCA chips (Fig. 1), so that even if one chip is blinded by a photon the other one can detect[5] the muon. In these two configurations the dead time is therefore determined by the pulse width ($\sim$25 ns) of the DIALOG chip. In the "one double-gap" configuration the muon is detected by a single CARIOCA chip (Fig. 1) which could be blinded by a photon detected in the double-gap considered. In that configuration the dead time is therefore determined by the pulse width ($\sim$50 ns) of the CARIOCA chip. The effect of the electronics dead time on the chamber efficiency in the three configurations was evaluated by a Monte Carlo simulation [22]. The chamber efficiency, measured with the

[4] The data reported in the lower curve were taken with the final gas mixture of $CO_2/Ar/CF_4$, 55/40/5% in volume. With this mixture the gain at 2.75 kV is $\sim$80% higher than that with the present gas.

[5] At the measured photon rate the probability that two photons blind simultaneously the two CARIOCAs is negligible.

Please cite this article as: M. Anelli, et al., Nucl. Instr. and Meth. A (2008), doi:10.1016/j.nima.2008.05.046

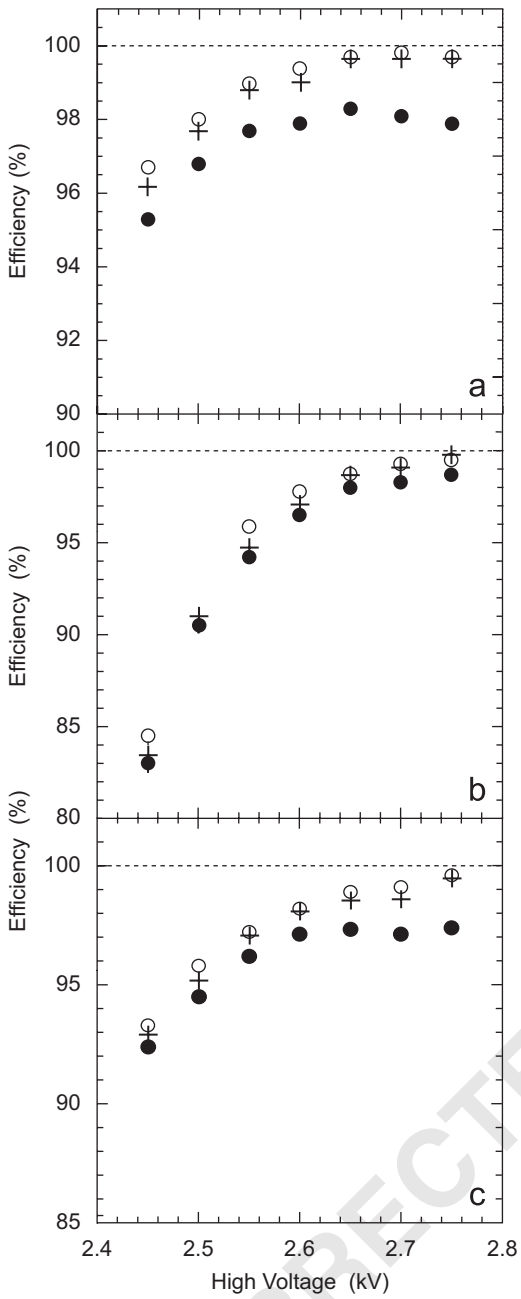

Fig. 4. Efficiency of the chamber in a 20 ns time window, as a function of the high voltage: (a) in the "four-gap" configuration; (b) in the "two single-gap" configuration; (c) in the "one double-gap" configuration. For each configuration the efficiency is measured with the source OFF (open circles), with the source ON and no dead time correction (full circles) and with source ON and dead time correction (crosses).

source ON (full circles in Fig. 4), was then corrected for this effect. The results reported in Fig. 4 (crosses) show that the decreased efficiency observed with the source ON can be fully ascribed to the dead time of the FEE. During the LHCb operation the highest rate forseen is about 200 kHz, in a logical channel belonging to a "two single-gap" chamber of region R4 in station M1 and the dead time effect is expected to be negligible.

3.2.2. Time resolution

The muon beam was monitored by a coincidence between the scintillation counters $S_1 - S_4$ (Fig. 2) which gives the common stop

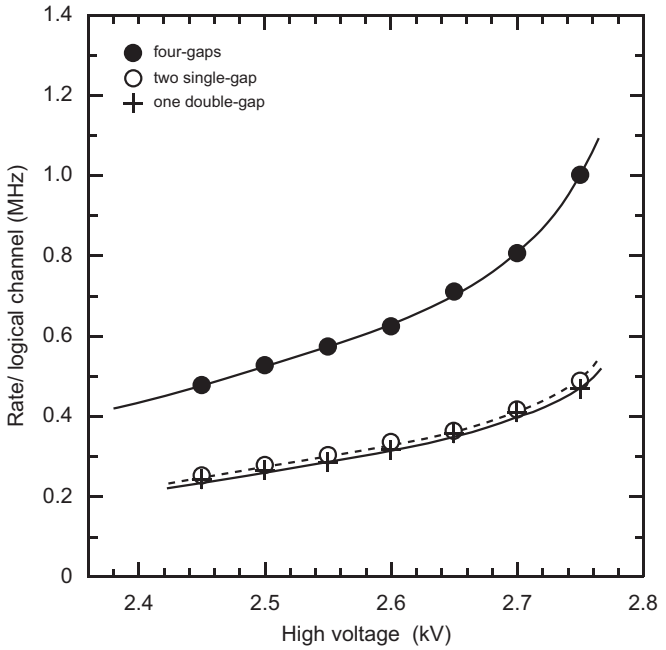

Fig. 5. Rate of a single logical channel as a function of the chamber high-voltage, when the chamber is exposed to the gamma flux. The photons detected in the four gaps are uncorrelated so that the rate in the "four-gap" configuration is twice that measured in the two "single-gap" and in the "one double-gap" configurations. The measured rates are of the same order of magnitude as those expected [23] at the LHC, in the most crowded chamber of the muon system.

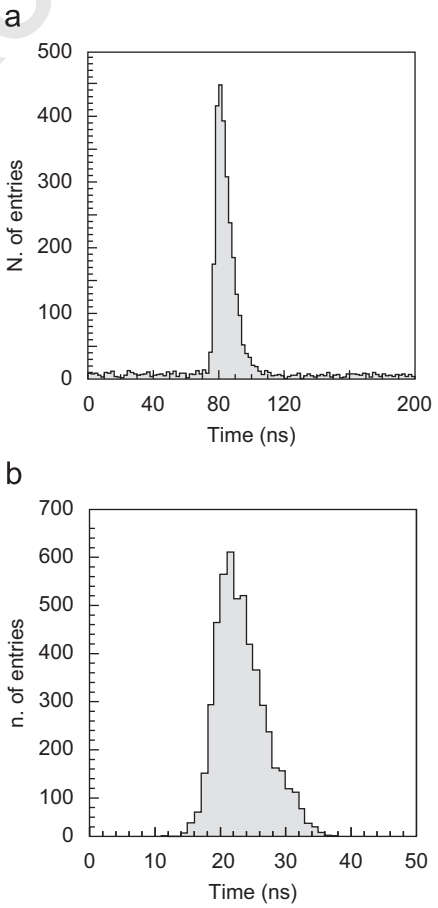

Fig. 6. Time distribution of the particles detected by the MWPC in the "four-gap" configuration: (a) with the source ON; (b) with the source OFF. In (a) all the hits recorded by the multihit TDC are included and the muon peak is superimposed on a flat background due to the detected photons. The zero of the time scales are

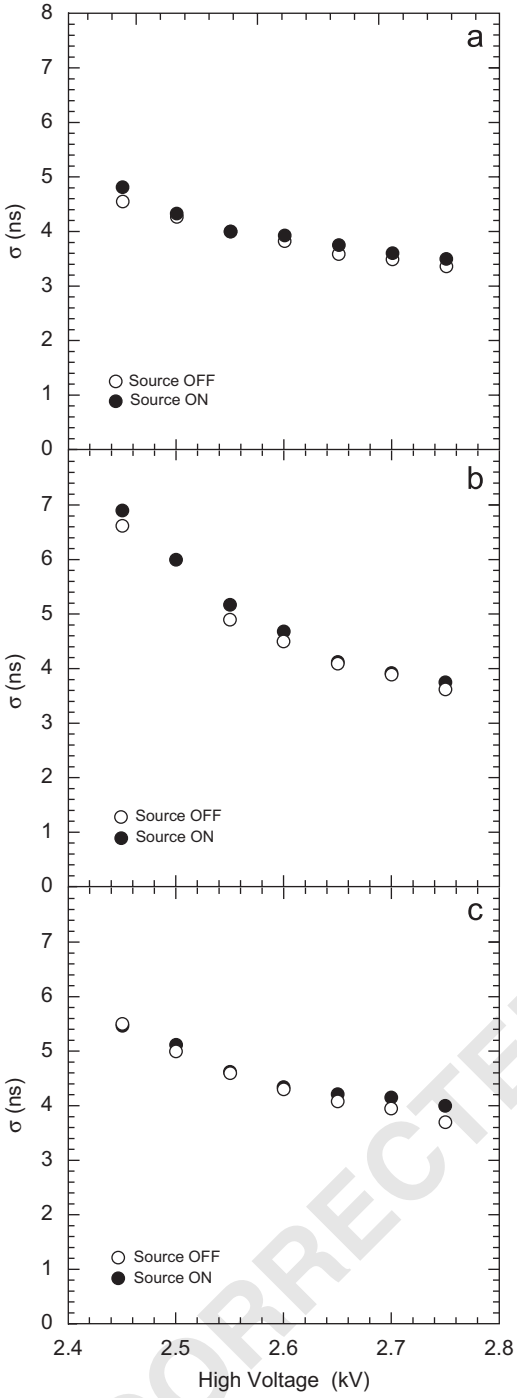

Fig. 7. Time resolution (standard deviation) of the MWPC with source ON and OFF: (a) in the "four-gap" configuration; (b) in the "two single-gap" configuration; (c) in the "one double-gap" configuration.

to several 16-channel multihit TDCs. The time jitter of this coincidence was estimated to be lower than 1 ns.

The start of the TDC channels is given by the logical channels of the chamber corresponding to the cathode pads crossed by the muon beam. A typical time distribution of the TDC, with the source ON, is reported in Fig. 6a for the "four-gap" configuration. In this chart a single event may contribute with many entries corresponding to photons or muons detected in a 200 ns interval. The main muon signal comes from the pad crossed by the muon, but in some cases the cross-talk signal from adjacent pads contributes to the spectrum of Fig. 6a with hits delayed by several ns with respect to the main muon signal. To eliminate this contribution, for each muon event only the hit closest to the mean time to the muon peak was retained. The time distribution obtained with the source OFF is reported in Fig. 6b. Similar time distribution were obtained with the chamber in the "two single-gap" and in the "one double-gap" configurations. From these distributions the time resolution of the chamber is obtained with the source ON and OFF. In Fig. 7 the time resolution is reported as a function of the HV, with the source OFF and ON and for the three chamber configurations. No noticeable effect of the gamma flux on the time resolution of the chamber and its FEE is observed.

4. Conclusions

A MWPC of the LHCb muon system was tested at the CERN Gamma Irradiation Facility (GIF). Three chamber configurations, corresponding to different HV settings of the anode wire planes, were investigated. The chamber, placed on a muon beam, was simultaneously exposed to the gamma flux coming from a 630 GBq ^{137}Cs source. The current drawn by the chamber and the output rate of the FEE during these tests were similar to those expected at the LHC in the most crowded chamber of the muon detector, with a luminosity of $2 \times 10^{32}\,\mathrm{cm}^{-2}/\mathrm{s}$ and no safety factor. The muon detection efficiency and time resolution were measured. No effect of the photon flux on the time resolution was found, while the observed decrease in the detection efficiency can be ascribed to the dead time of the FEE. These results give confidence that the expected performance of the muon wire chambers will be fulfilled.

Acknowledgments

We thank J.S. Graulich and B. Schmidt for their help in preparing the test.

References

[1] LHCb Collaboration, LHCb muon system, Technical Design Report, CERN-LHCC-2001-010, LHCb-TDR-4, 2001.
[2] LHCb Collaboration, Addendum to the Muon System Technical Design Report, CERN-LHCC-2003-002, LHCb-TDR-4-add-1, 2003.
[3] LHCb Collaboration, Second Addendum to the Muon System Technical Design Report, CERN-LHCC-2003-002, LHCb-TDR-4-add-2, 2005.
[4] G. Bencivenni, et al., Nucl. Instr. and Meth. A 513 (2003) 264.
[5] G. Bencivenni, et al., IEEE Trans. Nucl. Sci. NS-50 (2003) 1297.
[6] M. Alfonsi, et al., IEEE Trans. Nucl. Sci. NS-51 (2004) 2135.
[7] M. Alfonsi, et al., IEEE Trans. Nucl. Sci. NS-52 (2005) 2872.
[8] M. Alfonsi, et al., IEEE Trans. Nucl. Sci. NS-53 (2006) 322.
[9] M. Anelli, et al., IEEE Trans. Nucl. Sci. NS-53 (2006) 330.
[10] E. Dané, et al., IEEE Trans. Nucl. Sci. NS-54 (2007) 354.
[11] E. Dané, et al., Nucl. Instr. and Meth. A 572 (2007) 682.
[12] P. Ciambrone, et al., Nucl. Instr. and Meth. A 545 (2005) 156.
[13] S. Agosteo, et al., Nucl. Instr. and Meth. A 452 (2000) 94.
[14] "The Gamma Irradiation Facility," available from: ⟨http://ess.web.cern.ch/ESS/GIFProject/⟩.
[15] M. Anelli, "Chambers with cathode readout only," available from: ⟨http://indico.cern.ch/conferenceDisplay.py?confId=a03841⟩.
[16] M. Anelli, et al., LHCb Note, CERN-LHCb-2004-074, 2004.
[17] W. Bonivento, et al., Nucl. Instr. and Meth. A 491 (2002) 233.
[18] S. Cadeddu, et al., IEEE Trans. Nucl. Sci. NS-51 (2004) 1961.
[19] S. Cadeddu, et al., IEEE Trans. Nucl. Sci. NS-52 (2005) 2726.
[20] V. Bocci, et al., IEEE Nuclear Science Symposium Conference Record, vol. 3, 2007, p. 1737.
[21] V. Bocci, et al., IEEE Nuclear Science Symposium Conference Record, vol. 3, 2007, p. 2134.
[22] W. Riegler, LHCb Note CERN-LHCb-2000-060, 2005; W. Riegler, LHCb Note CERN-LHCb-2000-060, version 2, available from: ⟨http://indico.cern.ch/conferenceDisplay.py?confId=a03841⟩.
[23] G. Martellotti et al., LHCb Note CERN-LHCb-2005-075, 2005.
[24] I.B. Smirnov, Nucl. Instr. and Meth. A 554 (2005) 474;
I.B. Smirnov, CERN Comput. Newsl. 226 (1996) 13 available from: ⟨http://consult.cern.ch/writeups/heed/⟩.